Nanofiber-coated, tacrolimus-eluting sutures inhibit post-operative neointimal hyperplasia in rats

Kunal S. Parikh[a,b,c,d], **Aditya Josyula**[a,e], **Takahiro Inoue**[f], **Takuma Fukunishi**[f], **Huaitao Zhang**[f], **Revaz Omiadze**[a,c], **Richard Shi**[a,d], **Youseph Yazdi**[b,d], **Justin Hanes**[a,c,d,e,g,h,i,*], **Laura M. Ensign**[a,c,d,e,g,h,j,*], **Narutoshi Hibino**[f,k,**]

[a] Center for Nanomedicine, Johns Hopkins University School of Medicine, Baltimore, MD 21231, USA

[b] Center for Bioengineering Innovation & Design, Johns Hopkins University, Baltimore, MD 21218, USA

[c] Department of Ophthalmology, Wilmer Eye Institute, Johns Hopkins University School of Medicine, Baltimore, MD 21287, USA

[d] Department of Biomedical Engineering, Johns Hopkins University School of Medicine, Baltimore, MD 21205, USA

[e] Department of Chemical and Biomolecular Engineering, Johns Hopkins University, Baltimore, MD 21218, USA

[f] Department of Cardiac Surgery, Johns Hopkins University School of Medicine, Baltimore, MD 21287, USA

[g] Department of Pharmacology and Molecular Sciences, Johns Hopkins University School of Medicine, Baltimore, MD 21205, USA

[h] The Sidney Kimmel Comprehensive Cancer Center at Johns Hopkins University, Baltimore, MD 21231, USA

[i] Department of Neurosurgery, Johns Hopkins University School of Medicine, Baltimore, MD 21231, USA

[j] Department of Gynecology and Obstetrics and Division of Infectious Diseases, Johns Hopkins University School of Medicine, Baltimore, MD 21205, USA

[k] Department of Cardiac Surgery, University of Chicago/Advocate Children's Hospital, Chicago, IL 60637, USA

Abstract

[*] Corresponding authors at: 400 N. Broadway, 6017 Robert H. and Clarice Smith Building, Baltimore, MD 21231, USA. hanes@jhmi.edu (J. Hanes), lensign@jhmi.edu (L.M. Ensign). [**] Corresponding author at: 5841 S. Maryland Ave, Room E500B | MC5040, Chicago, IL 60637, USA. nhibino@surgery.bsd.uchicago.edu (N. Hibino).

Post-operative complications of vascular anastomosis procedures remain a significant clinical challenge and health burden globally. Each year, millions of anastomosis procedures connect arteries and/or veins in vascular bypass, vascular access, organ transplant, and reconstructive surgeries, generally via suturing. Dysfunction of these anastomoses, primarily due to neointimal hyperplasia and the resulting narrowing of the vessel lumen, results in failure rates of up to 50% and billions of dollars in costs to the healthcare system. Non-absorbable sutures are the gold standard for vessel anastomosis; however, damage from the surgical procedure and closure itself causes an inflammatory cascade that leads to neointimal hyperplasia at the anastomosis site. Here, we demonstrate the development of a novel, scalable manufacturing system for fabrication of high strength sutures with nanofiber-based coatings composed of generally regarded as safe (GRAS) polymers and either sirolimus, tacrolimus, everolimus, or pimecrolimus. These sutures provided sufficient tensile strength for maintenance of the vascular anastomosis and sustained drug delivery at the site of the anastomosis. Tacrolimus-eluting sutures provided a significant reduction in neointimal hyperplasia in rats over a period of 14 days with similar vessel endothelialization in comparison to conventional nylon sutures. In contrast, systemically delivered tacrolimus caused significant weight loss and mortality due to toxicity. Thus, drug-eluting sutures provide a promising platform to improve the outcomes of vascular interventions without modifying the clinical workflow and without the risks associated with systemic drug delivery.

Keywords

Suture; Nanofiber; Tacrolimus; Anastomosis; Vascular; Anti-proliferative

1. Introduction

Vascular anastomoses, or surgical connections between arteries and/or veins and vascular grafts, are one of the most commonly performed surgical procedures, involved in millions of vascular bypass, vascular access, solid organ transplant, and reconstruction procedures each year [1–5]. In each case, damage to the vessel walls during the surgical procedure, often using sutures, leads to deposition of platelets which release inflammatory chemokines and platelet-derived growth factor [6–8]. This cascade signals the inward migration and proliferation of smooth muscle cells, a process referred to as neointimal hyperplasia, resulting in thickening of the vessel wall [7,8]. The resulting narrowing of the vessel lumen (stenosis), is the major cause of arterial, venous, arteriovenous, and prosthetic graft failure [9–15]. Approximately 30% of all arterial bypass grafts and 50% of venous grafts fail due to neointimal hyperplasia [8]. Permanent vascular access is critical for patients with chronic kidney disease or end-stage renal disease undergoing hemodialysis. However, failure rates are reported as high as 50% in one year, and vascular access complications are responsible for 20% of patient hospitalizations [4,15,16]. There is a significant and unmet clinical need for vascular anastomosis with reduced complications, particularly with regard to post-operative neointimal hyperplasia.

Several alternative vascular anatomosis technologies have been developed over the past few decades, including clips, adhesives, lasers, sleeves, rings, stents, and other devices. However, each has its own limitations for use and/or associated complications, including

toxicity, leakage, occlusion, loss of strength, or the need to implant multiple devices [6,17–24]. Thus, non-absorbable nylon or polypropylene sutures remain the gold standard for anastomosis due to their convenience, reliability, flexibility, and capacity to provide strength at the anastomosis for an extended period of time [6]. Local delivery of anti-proliferative drugs such as sirolimus, tacrolimus, everolimus, or pimecrolimus via sutures may prevent neointimal hyperplasia, and therefore, improve surgical outcomes without modifying the clinical workflow [25]. The Cypher® sirolimus-eluting coronary stent demonstrated the clinical benefit of local anti-proliferative drug delivery by preventing restenosis following stent insertion into occluded vessels. In contrast to oral delivery of sirolimus, the Cypher® stent demonstrated superiority to bare metal coronary stents for an extended period of time at a lower drug dosage [26–31]. Over the past decade, interest in the development of drug-eluting sutures has grown with the objective of similarly providing local drug delivery at the surgical site to prevent complications and/or enhance wound healing. Literature reports have demonstrated delivery of a wide range of prophylactic and therapeutic moieties, including antibiotics, growth factors, anesthesia, and immunosuppressant agents [32–47]. However, clinical translation of such technologies has been curtailed due to an inability to (i) meet United States Pharmacopeia (U.S.P.) specifications for suture size and strength, (ii) provide sufficient and sustained drug delivery, and/or (iii) scale manufacturing to commercial viability [33,35,36,38,45–48]. Thus, to date, the only global market offerings are triclosan-coated sutures indicated for anti-infection applications in general surgery (U.S.P. sizes 6–0–1–0; 70–400 μm in diameter), and there are no smaller diameter drug-eluting sutures of the appropriate size for use in vascular surgery [49–52].

In order to provide for successful anastomosis while also preventing neointimal hyperplasia, a suture must: (i) surpass U.S.P. specifications for suture strength, and maintain strength at the anastomosis for an extended period of time; (ii) meet size requirements for sutures used in vascular surgery (U.S.P. sizes 9–0–7–0; 30–69 μm in diameter); (iii) provide delivery of therapeutic levels of an appropriate anti-proliferative drug; (iv) have potential for scaled manufacturing [53]. Here, we investigate the use of a novel electrospinning system to reproducibly manufacture drug-eluting, nanofibrous coatings for sutures [54]. Electrospinning is a manufacturing process in which high voltage is applied to a polymer or polymer/drug solution to draw out solid nanofibers or microfibers [55]. Specifically, we describe the manufacture of 8–0-sized, non-absorbable sutures with a 10–0 nylon core and nanofiber coating composed of poly(L-lactide) (PLLA), polyethylene glycol (PEG), and either sirolimus, tacrolimus, everolimus, or pimecrolimus. Originally used as an anti-fungal agent, sirolimus has been shown to be a potent anti-proliferative and anti-inflammatory drug which inhibits the mammalian target of sirolimus (mTOR) pathway [56]. Tacrolimus works as a calcineurin inhibitor, and has also demonstrated potent anti-proliferative and anti-inflammatory activity [36,47]. Everolimus and pimecrolimus are later generation analogs of sirolimus and tacrolimus, respectively, that have also been incorporated into drug-eluting stents [25]. PLLA and PEG are generally regarded as safe polymers (GRAS) that have been widely utilized in drug delivery applications, and are already incorporated in medical devices approved by the United States Food and Drug Administration [57]. We hypothesized that coating a non-absorbable, nylon suture with absorbable, drug-eluting nanofibers would simultaneously provide for sustained strength at the anastomosis and provide therapeutic

drug levels to facilitate optimal wound healing without neointimal hyperplasia. We investigate suture morphology, breaking strength, drug release, surgical anastomosis, and inhibition of neointimal hyperplasia in a rat model of vascular anastomosis.

2. Materials and methods

2.1. Materials

PLLA (221 kDa) was purchased from Corbion (Amsterdam, Netherlands). PEG (35 kDa), hexafluoroisopropanol, and formalin were procured from Sigma Aldrich (St. Louis, MO). Sirolimus, tacrolimus, everolimus, and pimecrolimus (each >99% purity) were purchased from LC Laboratories (Woburn, MA). 10–0 nylon sutures were obtained from either Ethicon (Somerville, NJ) or AROSurgical Instruments (Newport, CA). 1× Dulbecco's Phosphate-Buffered Saline (PBS) and Tween-20 were purchased from Fisher Scientific (Waltham, MA). Blocking reagent (Background Sniper) was purchased from Biocare Medical (Concord, CA). Anti-CD31 primary antibody (Ab28364) was procured from Abcam (Cambridge, MA) and species appropriate biotinylated secondary antibodies and Horseradish Peroxidase Streptavidin were purchased from Dako (Carpinteria, CA). 3,3-diaminobenzidine and hematoxylin counterstain (Gill's Formula) were obtained from Vector Laboratories (Burlingame, CA).

2.2. Suture fabrication

Polymer solutions were made via dissolution of PLLA, PEG, and sirolimus, tacrolimus, everolimus, or pimecrolimus in hexafluoroisopropanol by shaking overnight at room temperature. Polymer to solvent concentration was maintained at 10.8% (w/w) and PEG to PLLA concentration was maintained at 3.9% (w/w) for all formulations. Sirolimus concentration was 20%, 40%, or 80% (w/w) in regard to PLLA for the 20%, 40%, and 80% sirolimus/PLLA/PEG formulations, respectively. Tacrolimus, everolimus, and pimecrolimus concentration was 40% (w/w) in regard to PLLA for the 40% tacrolimus/PLLA/PEG, everolimus/PLLA/PEG, and pimecrolimus/PLLA/PEG formulations, respectively. Prior to electrospinning, the non-needled end of a 10–0 nylon suture was placed into the rotational collector. The needled end was driven through the hole in the opposing collector and allowed to hang loosely. Polymer/drug solutions were then pumped through a 20 G blunt-tip needle at 1 mL/h with an applied voltage of 15 kV at a distance of 17 cm from the parallel, grounded collectors. The collector containing the non-needled end of the suture was then rotated clockwise for 5 min at 150 rpm and counter-clockwise for 30 s at an identical speed in order to wrap the deposited nanofibers around the suture to form the nanofiber-coated sutures. The suture was then removed from the collectors and stored at − 20 °C. The sutures were classified as 8–0 Class II, non-absorbable surgical sutures by the U.S.P.

2.3. Suture characterization

2.3.1. Suture size—Suture diameter was determined via light microscopy (Eclipse TS100, Nikon Instruments, Melville, NY) and calibrated imaging software (Spot 5.2 Basic, Spot Imaging, Sterling Heights, MI). Each suture was measured at four different locations at least 2 cm apart, and used in further experimentation only if the average diameter was

between 40 and 49 μm and no individual measurement was lower than 35 μm or above 59 μm, qualifying as an 8–0-sized suture suitable for vascular surgery [53].

2.3.2.   Suture morphology—Nylon and nanofiber-coated suture morphology were observed via scanning electron microscopy (SEM) at 1 kV using a LEO Field Emission SEM (Zeiss, Oberkochen, Germany). All sutures were sputter coated with 10 nm of Au/Pd (Desk II, Denton Vacuum, Moorestown, NJ) prior to SEM.

2.3.3.   In vitro drug release and suture drug loading—To characterize the drug release rate from the drug-loaded nanofibers, 40% sirolimus, tacrolimus, everolimus, and pimecrolimus nanofibers were electrospun and twisted into 50 μm diameter fiber bundles ($n = 4$ for each condition). Fiber bundles were cut to 5 cm in length and submerged in 500 μL of PBS containing 2.5% (w/v) Tween-20 under sink conditions. Samples were placed on an orbital shaker at 37 °C, with the release medium collected and replenished with fresh media at 4 h, and at 1, 3, 5, 8, 11, and 14 days. Drug concentration within the release media was measured via high performance liquid chromatography (HPLC; Waters Corporation, Milford, MA) analysis. Samples were injected into a Phenomenex 100 C18 5 μm column (Phenomenex, Torrance, CA) within an oven at 30 °C. Sirolimus was detected at a wavelength of 268 nm using a mobile phase of water and methanol (19:81 v/v) at a flow rate of 1 mL/min for 10 mins. Tacrolimus was detected at a wavelength of 254 nm using a mobile phase of water and acetonitrile (17:83 v/v) at a flow rate of 1 mL/min for 10 mins. Everolimus was detected at a wavelength of 278 nm using a mobile phase of water and acetonitrile (17:83 v/v) at a flow rate of 1 mL/min for 10 mins. Pimecrolimus was detected at a wavelength of 210 nm using a mobile phase of water (buffered to pH 3 using hydrochloric acid) and acetonitrile (55:45 v/v) at a flow rate of 1 mL/min for 10 mins. Drug loading was determined by dissolving 1.5 cm of the fiber bundle in 1 mL of methanol followed by evaluation using the appropriate HPLC method for the specific drug.

2.3.4.   Breaking strength—10–0 nylon sutures were coated with 20% sirolimus, 40% sirolimus, 40% tacrolimus, 40% everolimus, or 40% pimecrolimus nanofibers ($n = 4$ for each condition) as described above. The resulting 8–0 sized sutures were tied into a surgeon's knot, clamped vertically, and pulled until breaking at a rate of 16 mm/min using a 5966 Dual Column Tabletop Testing System (Instron, Norwood, MA) [53]. The strength of vessels 14 days after anastomosis (described below) was also evaluated similarly by clamping the harvested vessel and pulling until its breaking point.

2.4.   Animal studies

All animals were cared for and experiments conducted in accordance with protocols approved by the Animal Care and Use Committee of the Johns Hopkins University, and in compliance with the National Institutes of Health guidelines for the Care and Use of Laboratory Animals.

Briefly, 8–12 week old female Lewis rats (Hilltop Lab Animals, Scottdale, PA and Harlan Laboratories, Frederick, MD) were anesthetized via intraperitoneal injection of ketamine (50 mg/kg) and xylazine (5 mg/kg), and kept under anesthesia with 2% isoflurane in

oxygen during the procedure. Female rats were utilized due to the potential for increased neointimal hyperplasia post-operatively [58]. A portion of the infrarenal abdominal aorta was exposed and cross-clamped, after which three-quarters of the circumference of the aorta was sectioned. The sectioned aorta was then repaired via interrupted suturing using 8–0 nylon, 40% sirolimus/nylon, 40% tacrolimus/nylon, 40% everolimus/nylon, or 40% pimecrolimus/nylon sutures ($n = 6$ for each condition), respectively. The suture coating remained intact throughout the suture handling process for each anastomosis procedure (not shown). The patency of the anastomosis and ensuing hemostasis were confirmed prior to closure of the abdomen. Animals were monitored daily for 14 days for signs of infection or irritation, after which the abdominal aorta was harvested and fixed in formalin for 24 h prior to sectioning and staining for analysis of neointimal hyperplasia and endothelialization. This animal model and endpoint were chosen because no significant additional progression in neointimal hyperplasia was observed afterwards, and they been previously used to investigate the effect of local drug delivery on post-anastomosis neointimal hyperplasia [48].

The same anastomosis procedure was utilized to characterize the relative efficacy and safety of systemically delivered tacrolimus. Following closure of the abdominal aorta using 8–0 nylon sutures, as described above, rats were divided into three groups, control ($n = 5$), daily low dose (1 mg/kg) tacrolimus ($n = 6$), and daily high dose (10 mg/kg) tacrolimus ($n = 12$). Drug was administered via intraperitoneal (IP) injection in 1 mL olive oil daily for 14 days. Control animals received injections of olive oil (vehicle) only. Rats were weighed daily and evaluated for gross signs of toxicity. At the study endpoint (14 days after anastomosis), 2–3 mL of blood was collected in tubes via cardiocentesis and submitted to the Clinical Pathology Phenotyping Core at Johns Hopkins University for analysis of markers of systemic toxicity, organs were weighed, and the abdominal aorta was harvested for analysis of neointimal hyperplasia.

The same anastomosis procedure was utilized to characterize blood vessel breaking strength 14 days after the procedure. The abdominal aorta was closed as described above using 8–0 nylon, 20% sirolimus/nylon, or 40% sirolimus/nylon sutures ($n = 5$, each). The patency of the anastomosis and ensuing hemostasis were confirmed prior to closure of the abdomen. Animals were monitored daily for 14 days for signs of infection or irritation, after which the aortas were harvested for immediate tensile strength testing as described above. A healthy, unoperated portion of the aorta was used for comparison (n = 5). All tissues were tested for breaking strength within 60 min of harvesting.

2.5. Evaluation of neointimal hyperplasia

Harvested tissue was embedded in paraffin, cross-sectioned, and stained with hematoxylin and eosin (H&E). Sections were taken in 5 μm increments proximal and distal to the visible central anastomosis site until suture cross-sections were no longer visible. Only sections containing sutures, indicating the anastomosis region, were utilized for evaluation of neointimal hyperplasia. The thickness of neointimal hyperplasia was measured using ImageJ (U.S. National Institutes of Health, Bethesda, MD, https://imagej.nih.gov/ij/) at three locations in each section and then averaged. The individual sections at the anastomosis site were then averaged together for each animal. Evaluation was masked for each condition,

although the nylon sutures remained within the tissue sections post staining. Due to the difference in the nylon suture cross-sectional thickness when comparing control nylon (8–0 core suture) and nanofiber-coated nylon (10–0 core suture), there were visible differences between control nylon versus drug-eluting sutures.

2.6. Immunohistochemistry

Following paraffin embedding and cross-sectioning, harvested tissue sections were deparaffinized, rehydrated, and blocked for endogenous peroxidase activity (0.3% H_2O_2 in MeOH) and nonspecific background staining (Background Sniper). Antigens were retrieved using the citrate buffer method (pH 6.0, 90 °C). Following incubation with primary antibodies (anti-CD31 (1:250, Ab28364)), binding was detected with species appropriate biotinylated secondary antibodies, incubation with Horseradish Peroxidase Streptavidin and chromogenic detection with 3,3-diaminobenzidine. Nuclei were identified via hematoxylin counterstain (Gill's Formula). Slides were then dehydrated, mounted, and evaluated. Four sections of each individual sample were counted at 40× (high powered field; HPF) and averaged for a total of six samples. Percent endothelialization was defined as the perimeter of the inner lumen stained CD31+ divided by the total inner lumen perimeter, as measured via ImageJ.

2.7. Statistical analysis

Breaking strength, drug release/loading, neointimal hyperplasia, percent endothelialization, percent weight change, and toxicity measures are presented as mean ± standard error. Statistical significance for these measurements was determined via one-way ANOVA followed by Tukey test. Statistical significance for rat survival was determined by the Mantel-Cox test. Statistical significance is shown as * $p < 0.05$, ** $p < 0.01$, or *** $p < 0.001$.

3. Results

3.1. Fabrication and characterization of nanofiber-coated sutures

In order to coat a standard nylon suture in a uniform, reproducible, and controlled manner, we designed a novel manufacturing system consisting of a syringe pump with a polymer/drug solution perpendicular to a pair of grounded collectors, one of which is capable of rotation [54]. The non-needled end of the nylon suture was attached to the collector capable of rotation, and the needled end of the suture was placed through the opposing collector (Fig. 1A). Drug-loaded polymer solutions were electrospun into nanofibers which deposited between the two parallel, grounded collectors, and were then twisted around the nylon suture by rotating the collector attached to the non-needled end of the suture.

Fig. 1B depicts a 10–0 nylon suture before (bottom) and after (top) coating with sirolimus-loaded nanofibers. Notably, electrospinning spray time can be adjusted in a facile manner to reproducibly modify coating thickness to meet suture diameter requirements (Table S1). SEM images displayed manufacture of non-porous, uniform nanofibers wound tightly around the nylon core to form a nanofiber-coated suture. Thin and short polymeric fibers were also dispersed around the outside of the coating. Fig. 1C depicts both the nylon

suture and coated nylon suture at a lower magnification, demonstrating the uniformity of the coating along the length of the suture. Control 8–0 nylon and 8–0 sized drug-eluting suture (10–0 nylon core) diameters are shown in Table S1 in the Supplementary Material.

3.2. In vitro release and loading of sirolimus, tacrolimus, everolimus, and pimecrolimus

The major challenge in the translation of drug-eluting sutures has been the inability to simultaneously surpass U.S.P. requirements for suture breaking strength while providing sufficient drug loading and sustained drug delivery. Thus, we next examined the drug release profiles and breaking strength of nanofiber-coated sutures. 20, 40, and 80% sirolimus nanofibers each demonstrated continued sirolimus release in vitro for at least 14 days (Fig. S1). However, the release profiles of each nanofiber formulation varied. The 20 and 40% formulations both demonstrated sustained release of sirolimus in vitro. However, as the concentration of drug within the nanofiber coating increased, a more pronounced burst effect was observed. In the case of the 80% sirolimus formulation, the majority of the sirolimus release occurred within the first 24 h (Fig. S1). Thus, to maximize the drug loading while also achieving sustained release, the 40% drug loading target was selected. The drug release profiles for each of the sirolimus, tacrolimus, everolimus, and pimecrolimus nanofibers is shown in Fig. 2. The release profiles for each drug were comparable, demonstrating a burst release initially, followed by continued release through day 14. Drug loading was also comparable for sirolimus (3.9 ± 0.2 μg/cm), tacrolimus (4.3 ± 0.4 μg/cm), everolimus (3.5 ± 0.3 μg/cm), and pimecrolimus (4.2 ± 0.1 μg/cm) sutures.

3.3. Nanofiber-coated suture breaking strength

We next evaluated the breaking strength of 10–0 nylon sutures coated with either 20 or 40% sirolimus nanofibers, or 40% tacrolimus, everolimus, or pimecrolimus nanofibers. According to the U.S.P., synthetic sutures resistant to the action of living mammalian tissue with a coating that adds significantly to suture diameter, but not to suture strength, are classified as Class II, non-absorbable surgical sutures [53]. The coating process used in this study increased the size of a standard 10–0 nylon suture to 46–49 um, classified as 8–0 sutures. The minimum average knot-pull tensile strength requirement for an 8–0, non-absorbable, Class II suture is 0.39 N [53]. As shown in Fig. 3, all nanofiber-coated suture formulations surpassed U.S.P. specifications for suture breaking strength by more than 30%. Moreover, because suture strength was derived from the 10–0 nylon core, doubling the concentration of sirolimus within the coating formulation (20% vs 40%) did not significantly affect suture strength. Additionally, there was no significant change in breaking strength with change in drug (Fig. 3), demonstrating the robustness of the platform.

3.4. Effect of anti-inflammatory nanofiber coatings on post-operative neointimal hyperplasia

We evaluated the potential clinical utility of anti-inflammatory, nanofiber-coated nylon sutures by determining their capacity to maintain an anastomosis and inhibit neointimal hyperplasia. The rat abdominal aorta was anastomosed using either 8–0 nylon or 10–0 nylon sutures coated with 40% sirolimus, tacrolimus, everolimus, or pimecrolimus-eluting nanofibers to make 8–0 sized drug-eluting sutures. No suture-related or other complications were observed during any of the procedures. The nanofiber-coated nylon sutures were

able to pass through the tissue several times and suture the vessel appropriately without any peeling or loss of the coating (not shown). Further, vessel patency and hemostasis were visually confirmed immediately post-operatively in all cases. No anti-platelet or anti-coagulation therapy, or any other kind of therapy was provided in the post-operative period, and there was no operative or suture-related infection or mortality at any time under any suture condition. In fact, we found that there was no significant difference in vessel breaking strength between healthy control vascular tissue, or vascular tissue closed with nylon or sirolimus-eluting sutures 14 days after the anastomosis procedure (Fig. S2). After 14 days, rat abdominal aortas were harvested and evaluated grossly and via histology. In all cases, the sutures remained in place, and there was no leakage observed visually at the anastomosis. Masson's trichrome staining of tissue sections at the anastomosis allowed for measurement of neointimal hyperplasia (Fig. 4A) within the inner lumen of vessels sutured using nylon (Fig. 4B), 40% sirolimus (Fig. 4C), 40% tacrolimus (Fig. 4D), 40% everolimus (Fig. 4E), or 40% pimecrolimus (Fig. 4F) sutures, indicated by a highly inflamed, pink-colored tissue region. There was a non-significant trend in reduction in neointimal hyperplasia in rats receiving sirolimus-eluting sutures (205.5 ± 2.6 μm) in comparison to rats receiving nylon sutures (226.8 ± 9.1 μm) ($p = 0.34$) (Fig. 4A). There was a significant reduction in neointimal hyperplasia thickness in tissues anastomosed using tacrolimus- (176.8 ± 4.8 μm), everolimus- (175.3 ± 14.5 μm), and pimecrolimus-eluting sutures (181.7 ± 8.1 μm) in comparison to vessels sutured using the standard nylon suture ($p < 0.01$). Further, 40% tacrolimus sutures significantly decreased neointimal hyperplasia in comparison to 40% sirolimus sutures ($p < 0.01$), and reduced neointimal hyperplasia by 22% in comparison to the rats with conventional nylon sutures.

3.5. Effect of anti-inflammatory nanofiber coatings on vessel endothelialization

In order to characterize the effect of local anti-proliferative drug delivery on post-operative vessel healing, CD31 staining was used as a marker of endothelialization. While 40% everolimus and pimecrolimus sutures were associated with a trend toward increased percent endothelialization 14 days after the anastomosis, there was no significant difference in endothelialization across suture conditions (Fig. 5A). Single layers of CD31+ cells were present at the inner lumen of vessels anastomosed via each suture type (Fig. 5B–F), indicating that local drug release did not suppress post-operative endothelialization compared to nylon sutures alone. Notably, immunohistochemistry images showed CD31+ cells directly adjacent to each suture type.

3.6. Evaluation of the safety and efficacy of systemic tacrolimus administration

Due to its increased effectiveness in comparison to either a nylon or sirolimus suture, tacrolimus was selected for additional evaluation. In order to characterize the potential benefit of local tacrolimus delivery via sutures in comparison to systemic delivery, we also delivered tacrolimus daily via IP injection in rats receiving a nylon suture. Body weight, survival, neointimal hyperplasia, and several blood markers were evaluated for rats in the control (nylon suture + daily IP injection of vehicle), low dose tacrolimus (nylon suture + daily IP injection of 1 mg/kg tacrolimus), and high dose tacrolimus (nylon suture + daily IP injection of 10 mg/kg tacrolimus) groups. Low and high dose concentrations were selected based on the spectrum of tacrolimus doses previously investigated in rats via

IP administration [59–61]. The average body weight of rats in each group decreased at post-operative day 1; however, the average weight of rats in the control (1.4% total increase to 216 ± 2.9 g) and low dose (3.9% total decrease to 208 ± 1.8 g) groups recovered over the 14-day post-operative period. In comparison, the average weight of the surviving rats in the high dose group decreased by 17% to 186 ± 15 g at 14 days, indicating that the treatment was not well-tolerated (Fig. 6A). 100% of rats receiving the control (5/5) and low dose treatments (6/6) survived in comparison to only 25% of rats receiving the high dose treatment (3/12) (Fig. 6B). In addition to significant body weight reduction and death, the high tacrolimus dose also led to significant decrease in spleen and kidney weight, as well as decreased total blood protein concentration (Tables S2–S3). The high dose tacrolimus treatment provided a significant reduction in neointimal hyperplasia thickness by 17% to 180.8 μm in the three rats that survived to the 14-day endpoint ($p < 0.05$) (Fig. 6C). In contrast, the low dose tacrolimus treatment, while better tolerated than the high dose, had no effect on neointimal hyperplasia (Fig. 6C). Demonstrating the benefit of local drug delivery, the 40% tacrolimus-eluting sutures were able to provide a significant reduction in neointimal hyperplasia by 22% to 176.8 μm (Fig. 5), while maintaining 100% survival (6/6) at approximately 25-fold lower tacrolimus dose than the daily low dose IP tacrolimus treatment.

4. Discussion

The local vascular smooth muscle cell population is multiplied up to five times in the 14 days following vascular anastomosis procedures [7]. This post-operative inflammatory response contributes to 90% of the total neointimal hyperplasia, and the resulting stenosis can have devastating consequences, including re-operation, graft/transplant failure, and death [4,7,14,16]. Thus, it is critical to modulate the local, post-operative biological response in order to improve the outcomes of arterial, venous, arteriovenous, and prosthetic graft procedures. We developed a new method to endow conventional sutures with drug delivery functionality via a nanofiber coating, and evaluated its potential for use in vascular anastomosis procedures. This method allowed for facile specification of nanofiber coating thickness and tuning of drug release profiles. Nanofiber coatings demonstrated uniformity along the length of the suture and remained intact while suturing in vivo. Importantly, nanofiber-coated sutures met or exceeded U.S.P. specifications for 8–0 suture diameter and strength, respectively, allowing for clinical translation. Tacrolimus-eluting sutures significantly reduced neointimal hyperplasia in comparison to a standard 8–0 nylon suture following anastomosis of the abdominal aorta in rats, and demonstrated improved safety compared to systemically (IP) dosed tacrolimus.

Sirolimus, tacrolimus, everolimus, and pimecrolimus were chosen for this study due to their extensive use, well-known mechanisms of action, and demonstrated ability to reduce neointimal hyperplasia in various models [7,17,20,27,28]. However, there has been a concern that while the anti-proliferative activity of these small molecules may inhibit neointimal hyperplasia, it may also inhibit appropriate endothelialization and healing at the anastomosis [36]. In this study, tacrolimus, everolimus, and pimecrolimus-eluting suture conditions demonstrated a significant reduction in neointimal hyperplasia while also mechanically maintaining the vascular anastomosis through the duration of the study. We

found no significant difference in the breaking strength of healthy rat vessels and vessels closed with nylon or sirolimus-eluting sutures 14 days after the anastomosis procedure. Moreover, endothelialization occurred in each of the anastomosed vessels, regardless of suture type, and CD31+ cell layers were found directly adjacent to anti-proliferative sutures. Thus, it appears that the capacity of the nanofiber coatings to deliver low levels of drug in a sustained manner may provide sufficient modulation of the post-operative inflammatory response while also allowing for appropriate vessel healing.

In addition, major advantages of this platform are the versatility of electrospinning to incorporate a range of different drugs and polymers, and that the core nylon suture provides the required tensile strength [62]. Thus, a wide range of polymer/drug formulations could be explored to achieve the appropriate release of the active agent in a manner that both significantly reduces neointimal hyperplasia and stenosis while promoting long-term vascular health. This versatility may also allow for incorporation of multiple types of fibers into a single, tightly wound coating. For example, a coating composed of both short- and long-term degradation fibers could be used to provide early- and extended-term drug release to prevent both immediate- and late-stage complications. While our studies demonstrated that delivery of anti-proliferative agents in the early post-operative period may improve outcomes, local delivery of these agents may be useful for as long as a suture or prosthetic graft remains present at the anastomosis [6–8]. The use of this highly versatile and tunable coating platform as a research tool may help to further elucidate the types of drugs and release profiles that are conducive to realizing both objectives.

Previous studies have explored various methods of local drug delivery at the anastomosis site, including dip-coated sutures, nanofiber wool, films, and gels [17,20,22,36,46]. Notably, in the cases of films, gels, and wool, an additional closure device is required in order to perform and maintain the anastomosis. Although the animal models tested have varied significantly in the literature (e.g., anastomosis site, closure method, number of sutures used), in each case, local delivery of anti-proliferative agents, including tacrolimus, has significantly reduced neointimal hyperplasia. Our approach to drug delivery allowed for increased drug loading at the anastomosis site within a suture meeting size and strength specifications and providing convenience for clinical use [22,36,46]. To our knowledge, this is the first study to directly compare multiple generations of anti-proliferative drugs (sirolimus and tacrolimus vs everolimus and pimecrolimus, respectively) with differing mechanisms of actions in the same model of vascular anastomosis-induced neointimal hyperplasia. Interestingly, although tacrolimus has been shown to have reduced anti-proliferative potency and less inhibitory effects on endothelialization in comparison to sirolimus, in this study, tacrolimus significantly reduced neointimal hyperplasia, but there was no significant change in percent endothelialization [63]. Notably, only tacrolimus-, everolimus-, and pimecrolimus-eluting sutures significantly reduced neointimal hyperplasia in comparison to conventional nylon sutures. The suboptimal effect of sirolimus was hypothesized in comparison to more effective later generation analogs, such as everolimus; however, it is possible that further optimization of sirolimus loading and release could provide for improved efficacy [64]. For example, the increased drug loading of the tacrolimus-eluting suture in comparison to the sirolimus suture may have contributed to its effectiveness.

There are several potential limitations in the study and in the evaluation of the suture technology described here. Although the high dose tacrolimus group demonstrated a significant reduction in neointimal hyperplasia in comparison to a control vessel, the sample size was limited as only three rats from the high dose tacrolimus group survived through day 14. Similarly, although the reduction in neointimal hyperplasia due to everolimus- and pimecrolimus-eluting sutures was not significant in comparison to sirolimus, it is possible that a larger group size would have led to statistical significance. Finally, additional investigation of suture drug loading and release profile for each drug may have further improved suture performance. Future studies should include dose ranging studies and various drug release profiles in order to further reduce of neointimal hyperplasia and promotion of endothelialization. In addition, although the nanofiber-coated nylon sutures described in this study surpassed U.S.P. requirements for suture strength and maintained the anastomosis for at least 14 days, it is important to note that the U.S.P. only specifies a minimum average suture breaking strength. Prior to clinical studies, it will be important to evaluate the durability of nanofiber-coated sutures in large animal models and in different types of anastomosis procedures for a longer duration to ensure that they maintain the anastomosis. Longer-term studies may also further elucidate the differences in endothelialization due to each drug. If successful, nanofiber-coated sutures may have significant potential for use in vascular anastomosis procedures due to their capacity to effectively reduce neointimal hyperplasia without changing the surgical procedure or clinical workflow.

5. Conclusions

This study demonstrated the manufacture of nanofiber-coated nylon sutures capable of meeting U.S.P. specifications for suture size and strength for vascular surgery, maintaining an in vivo surgical anastomosis, and providing sustained release of mTOR or calcineurin inhibitors without preventing endothelialization in a rat vascular anastomosis model. In addition, local delivery of tacrolimus via the suture significantly reduced post-operative neointimal hyperplasia. In contrast, achieving a comparable level of reduction via systemic tacrolimus administration resulted in significant mortality (25% survival rate). This platform has the potential to reduce post-operative complications and improve the clinical outcomes following vascular bypass and vascular access surgeries, which present a significant economic and health burden, without modifying the current surgical workflow.

Supplementary Material

Refer to Web version on PubMed Central for supplementary material.

Acknowledgements

Data availability

Data will be made available on request.

References

[1]. Kellar CA, Solid organ transplantation overview and selection criteria, Am. J. Manag. Care 21 (1 Suppl) (2015) S4–11.

[2]. Goodney PP, Beck AW, Nagle J, Welch HG, Zwolak RM, National trends in lower extremity bypass surgery, endovascular interventions, and major amputations, J. Vasc. Surg. 50 (1) (2009) 54–60. [PubMed: 19481407]

[3]. Abu-Omar Y, Taggart DP, Coronary artery bypass surgery, Medicine 42 (9) (2014) 527–531.

[4]. Lok CE, Foley R, Vascular access morbidity and mortality: trends of the last decade, Clin. J. Am. Soc. Nephrol. 8 (7) (2013) 1213–1219. [PubMed: 23824198]

[5]. Browning MB, Dempsey D, Guiza V, Becerra S, Rivera J, Russell B, Höök M, Clubb F, Miller M, Fossum T, Dong JF, Bergeron AL, Hahn M, Cosgriff-Hernandez E, Multilayer vascular grafts based on collagen-mimetic proteins, Acta Biomater. 8 (3) (2012) 1010–1021. [PubMed: 22142564]

[6]. Zeebregts CJ, Non-penetrating clips for vascular anastomosis, Eur. J. Vasc. Endovasc. Surg. 30 (3) (2005) 288–290. [PubMed: 15893485]

[7]. Marx SO, Totary-Jain H, Marks AR, Vascular smooth muscle cell proliferation in restenosis, Circulation, Cardiovasc. Interv. 4 (1) (2011) 104–111.

[8]. Han J, Lelkes PI, Drug-eluting vascular grafts, in: Domb AJ, Khan W (Eds.), Focal Controlled Drug Delivery, Springer, US, Boston, MA, 2014, pp. 405–427.

[9]. Ogus TN, Basaran M, Selimoglu O, Yildirim T, Ogus H, Ozcan H, Us MH, Long-term results of the left anterior descending coronary artery reconstruction with left internal thoracic artery, Ann. Thorac. Surg. 83 (2) (2007) 496–501. [PubMed: 17257976]

[10]. Souza DS, Johansson B, Bojo L, Karlsson R, Geijer H, Filbey D, Bodin L, Arbeus M, Dashwood MR, Harvesting the saphenous vein with surrounding tissue for CABG provides long-term graft patency comparable to the left internal thoracic artery: results of a randomized longitudinal trial, J. Thorac. Cardiovasc. Surg. 132 (2) (2006) 373–378. [PubMed: 16872965]

[11]. Mack MJ, Osborne JA, Shennib H, Arterial graft patency in coronary artery bypass grafting: what do we really know? Ann. Thorac. Surg. 66 (3) (1998) 1055–1059. [PubMed: 9769002]

[12]. Roy-Chaudhury P, Kelly BS, Zhang J, Narayana A, Desai P, Melham M, Duncan H, Heffelfinger SC, Hemodialysis vascular access dysfunction: from pathophysiology to novel therapies, Blood Purif. 21 (1) (2003) 99–110. [PubMed: 12596755]

[13]. Kapadia MR, Popowich DA, Kibbe MR, Modified prosthetic vascular conduits, Circulation 117 (14) (2008) 1873–1882. [PubMed: 18391121]

[14]. Towbin AJ, Towbin RB, Di Lorenzo C, Grifka RG, Interventional radiology in the treatment of the complications of organ transplant in the pediatric population—part 1: the kidneys, heart, lungs, and intestines, Semin. Interv. Radiol. 21 (4) (2004) 309–320.

[15]. Pantelias K, Grapsa E, Vascular access today, World J. Nephrol 1 (3) (2012) 69–78. [PubMed: 24175244]

[16]. Li L, Terry CM, Shiu Y-TE, Cheung AK, Neointimal hyperplasia associated with synthetic hemodialysis grafts, Kidney Int. 74 (10) (2008) 1247–1261. [PubMed: 18668026]

[17]. Schachner T, Zou Y, Oberhuber A, Tzankov A, Mairinger T, Laufer G, Bonatti JO, Local application of rapamycin inhibits neointimal hyperplasia in experimental vein grafts, Ann. Thorac. Surg. 77 (5) (2004) 1580–1585. [PubMed: 15111146]

[18]. Paulson WD, Kipshidze N, Kipiani K, Beridze N, DeVita MV, Shenoy S, Iyer SS, Safety and efficacy of local periadventitial delivery of sirolimus for improving hemodialysis graft patency: first human experience with a sirolimus-eluting collagen membrane (Coll-R), Nephrol. Dial. Transplant. 27 (3) (2012) 1219–1224. [PubMed: 22241793]

[19]. Manson RJ, Ebner A, Gallo S, Chemla E, Mantell M, Deaton D, Roy-Chaudhury P, Arteriovenous fistula creation using the optiflow vascular anastomosis device: a first in man pilot study, Semin. Dial. 26 (1) (2013) 97–99. [PubMed: 22486998]

[20]. Kawatsu S, Oda K, Saiki Y, Tabata Y, Tabayashi K, External application of rapamycin-eluting film at anastomotic sites inhibits neointimal hyperplasia in a canine model, Ann. Thorac. Surg. 84 (2) (2007) 560–567, discussion 567. [PubMed: 17643635]

[21]. Chang EI, Galvez MG, Glotzbach JP, Hamou CD, El-ftesi S, Rappleye CT, Sommer K-M, Rajadas J, Abilez OJ, Fuller GG, Longaker MT, Gurtner GC, Vascular anastomosis using controlled phase transitions in poloxamer gels, Nat. Med. 17 (9) (2011) 1147–1152. [PubMed: 21873986]

[22]. Mutsuga M, Narita Y, Yamawaki A, Satake M, Kaneko H, Usui A, Ueda Y, Development of novel drug-eluting biodegradable nano-fiber for prevention of postoperative pulmonary venous obstruction, Interact. Cardiovasc. Thorac. Surg. 8 (4) (2009) 402–407. [PubMed: 19139028]

[23]. Takenaka H, Esato K, Ohara M, Zempo N, Sutureless anastomosis of blood vessels using cyanoacrylate adhesives, Surg. Today 22 (1) (1992) 46–54. [PubMed: 1547375]

[24]. Chang DW, Chan A, Forse RA, Abbott WM, Enabling sutureless vascular bypass grafting with the exovascular sleeve anastomosis, J. Vasc. Surg. 32 (3) (2000) 524–530. [PubMed: 10957659]

[25]. Tamburino C, Capodanno D, Evolution of stents: past, present and future, Expert. Rev. Cardiovasc. Ther. 7 (5) (2009) 443–446. [PubMed: 19419249]

[26]. Colombo A, Orlic D, Stankovic G, Corvaja N, Spanos V, Montorfano M, Liistro F, Carlino M, Airoldi F, Chieffo A, Preliminary observations regarding angiographic pattern of restenosis after rapamycin-eluting stent implantation, Circulation 107 (17) (2003) 2178–2180. [PubMed: 12719283]

[27]. Toutouzas K, Di Mario C, Falotico R, Takagi T, Stankovic G, Albiero R, Corvaja N, Colombo A, Sirolimus-eluting stents: a review of experimental and clinical findings, Z. Kardiol. 91 (Suppl. 3) (2002) 49–57.

[28]. Suzuki T, Kopia G, Hayashi S, Bailey LR, Llanos G, Wilensky R, Klugherz BD, Papandreou G, Narayan P, Leon MB, Yeung AC, Tio F, Tsao PS, Falotico R, Carter AJ, Stent-based delivery of sirolimus reduces neointimal formation in a porcine coronary model, Circulation 104 (10) (2001) 1188–1193. [PubMed: 11535578]

[29]. Rodriguez AE, Granada JF, Rodriguez-Alemparte M, Vigo CF, Delgado J, Fernandez-Pereira C, Pocovi A, Rodriguez-Granillo AM, Schulz D, Raizner AE, Palacios I, O'Neill W, Kaluza GL, Stone G, Oral rapamycin after coronary baremetal stent implantation to prevent restenosis: the Prospective, Randomized Oral Rapamycin in Argentina (ORAR II) Study, J. Am. Coll. Cardiol. 47 (8) (2006) 1522–1529. [PubMed: 16630986]

[30]. Stojkovic S, Ostojic M, Nedeljkovic M, Stankovic G, Beleslin B, Vukcevic V, Orlic D, Arandjelovic A, Kostic J, Dikic M, Tomasevic M, Systemic rapamycin without loading dose for restenosis prevention after coronary bare metal stent implantation, Catheter. Cardiovasc. Interv. 75 (3) (2010) 317–325. [PubMed: 20049961]

[31]. Gershlick AH, Is there any place for oral anti-restenotic treatment in the era of drug eluting stents? Heart 91 (11) (2005) 1377–1379. [PubMed: 16230428]

[32]. Wen Hu, Huang Zheng-Ming, Liu X-Y, Development of braided drug-nanofiber sutures, Nanotechnology 21 (2010) 1–11.

[33]. Weldon CB, Tsui JH, Shankarappa SA, Nguyen VT, Ma M, Anderson DG, Kohane DS, Electrospun drug-eluting sutures for local anesthesia, J. Control. Release 161 (3) (2012) 903–909. [PubMed: 22609349]

[34]. Pasternak B, Rehn M, Andersen L, Ågren M, Heegaard A-M, Tengvall P, Aspenberg P, Doxycycline-coated sutures improve mechanical strength of intestinal anastomoses, Int. J. Color. Dis. 23 (3) (2008) 271–276.

[35]. Obermeier A, Schneider J, Wehner S, Matl FD, Schieker M, von Eisenhart-Rothe R, Stemberger A, Burgkart R, Novel high efficient coatings for anti-microbial surgical sutures using chlorhexidine in fatty acid slow-release carrier systems, PLoS One 9 (7) (2014), e101426. [PubMed: 24983633]

[36]. Morizumi S, Suematsu Y, Gon S, Shimizu T, Inhibition of neointimal hyperplasia with a novel tacrolimus-eluting suture, J. Am. Coll. Cardiol. 58 (4) (2011) 441–442. [PubMed: 21757126]

[37]. Mack BC, Wright KW, Davis ME, A biodegradable filament for controlled drug delivery, J. Control. Release 139 (3) (2009) 205–211. [PubMed: 19567255]

[38]. Lee JE, Park S, Park M, Kim MH, Park CG, Lee SH, Choi SY, Kim BH, Park HJ, Park JH, Heo CY, Choy YB, Surgical suture assembled with polymeric drug-delivery sheet for sustained, local pain relief, Acta Biomater. 9 (9) (2013) 8318–8327. [PubMed: 23770220]

[39]. Joseph J, Nair SV, Menon D, Integrating substrateless electrospinning with textile technology for creating biodegradable three-dimensional structures, Nano Lett. 15 (8) (2015) 5420–5426. [PubMed: 26214718]

[40]. Hu W, Huang ZM, Liu XY, Development of braided drug-loaded nanofiber sutures, Nanotechnology 21 (31) (2010), 315104. [PubMed: 20622298]

[41]. Hu W, Huang Z-M, Biocompatibility of braided poly(L-lactic acid) nanofiber wires applied as tissue sutures, Soc. Chem. Ind. 59 (2010) 92–99.

[42]. He CL, Huang ZM, Han XJ, Fabrication of drug-loaded electrospun aligned fibrous threads for suture applications, J. Biomed. Mater. Res. A 89 (1) (2009) 80–95. [PubMed: 18428982]

[43]. Catanzanoa O, Aciernob S, Russo P, Cervasio M, Del Basso De M, Caro A, Bolognesee G, Sammartino L, Califano G, Marenzi A, Calignano D, Quaglia Acierno F, Melt-spun bioactive sutures containing nanohybrids for local delivery of anti-inflammatory drugs, Mater. Sci. Eng. C 43 (2014) 300–309.

[44]. Choudhury AJ, Gogoi D, Chutia J, Kandimalla R, Kalita S, Kotoky J, Chaudhari YB, Khan MR, Kalita K, Controlled antibiotic-releasing Antheraea assama silk fibroin suture for infection prevention and fast wound healing, Surgery 159 (2) (2015) 539–547. [PubMed: 26328475]

[45]. Kashiwabuchi F, Parikh KS, Omiadze R, Zhang S, Luo L, Patel HV, Xu Q, Ensign LM, Mao H-Q, Hanes J, McDonnell PJ, Development of absorbable, antibiotic-eluting sutures for ophthalmic surgery, Transl. Vision Sci. Technol. 6 (1) (2017), 1–1.

[46]. Ak K, Ak E, Dericioglu O, Canak T, Akbuga J, Ozkan N, Cetinel S, Isbir S, Arsan S, Cobanoglu A, Tacrolimus-eluting suture inhibits neointimal hyperplasia: an experimental in vivo study in rats, Eur. J. Vasc. Endovasc. Surg. 53 (3) (2017) 431–437. [PubMed: 28065442]

[47]. Hamada N, Miyata M, Eto H, Shirasawa T, Akasaki Y, Nagaki A, Tei C, Tacrolimus-eluting stent inhibits neointimal hyperplasia via calcineurin/NFAT signaling in porcine coronary artery model, Atherosclerosis 208 (1) (2010) 97–103. [PubMed: 19682688]

[48]. Mutsuga M, Narita Y, Yamawaki A, Satake M, Kaneko H, Suematsu Y, Usui A, Ueda Y, A new strategy for prevention of anastomotic stricture using tacrolimus-eluting biodegradable nanofiber, J. Thorac. Cardiovasc. Surg. 137 (3) (2009) 703–709. [PubMed: 19258093]

[49]. Marco Fernando, Vallez Raquel, Gonzalez Pablo, Ortega Luis, De La Lama Jose, Lopez-Duran L, Study of the efficacy of coated Vicryl plus® antibacterial suture in an animal model of orthopedic surgery*, Surg. Infect. 8 (2007) 359–365.

[50]. Ming X, Nichols M, Rothenburger S, In vivo antibacterial efficacy of MONOCRYL plus antibacterial suture (Poliglecaprone 25 with triclosan), Surg. Infect. 8 (2) (2007) 209–214.

[51]. Ming X, Rothenburger S, Yang D, In vitro antibacterial efficacy of MONOCRYL plus antibacterial suture (Poliglecaprone 25 with triclosan), Surg. Infect. 8 (2) (2007) 201–208.

[52]. Ming Xintian, Rothenberger Stephen, Nichols M, In vivo and in vitro antibacterial efficacy of PDS* plus (Polidioxanone with Triclosan) suture, Surg. Infect. 9 (2008) 451–458.

[53]. The United States Pharmacopeial Convention, USP 29-NF 24. (Rockville, MD: The United States Pharmacopeial Convention, January 1, 2006) 2052, 2022.

[54]. Parikh KS, Omiadze R, Josyula A, Shi R, Anders NM, He P, Yazdi Y, McDonnell PJ, Ensign LM, Hanes J, Ultra-Thin, High Strength, Antibiotic-Eluting Sutures for Prevention of Ophthalmic Infection, Bioeng. Transl. Med. 6 (2021) e10204. [PubMed: 34027091]

[55]. Bhardwaj N, Kundu SC, Electrospinning: a fascinating fiber fabrication technique, Biotechnol. Adv. 28 (3) (2010) 325–347. [PubMed: 20100560]

[56]. Fingar DC, Richardson CJ, Tee AR, Cheatham L, Tsou C, Blenis J, mTOR controls cell cycle progression through its cell growth effectors S6K1 and 4E-BP/eukaryotic translation initiation factor 4E, Mol. Cell. Biol. 24 (1) (2004) 200–216. [PubMed: 14673156]

[57]. Ulery BD, Nair LS, Laurencin CT, Biomedical applications of biodegradable polymers, J. Polym. Sci. B Polym. Phys. 49 (12) (2011) 832–864. [PubMed: 21769165]

[58]. Robinet P, Milewicz DM, Cassis LA, Leeper NJ, Lu HS, Smith JD, Consideration of sex differences in design and reporting of experimental arterial pathology studies-statement from ATVB council, Arterioscler. Thromb. Vasc. Biol. 38 (2) (2018) 292–303. [PubMed: 29301789]

[59]. Akar Y, Yucel G, Durukan A, Yucel I, Arici G, Systemic toxicity of tacrolimus given by various routes and the response to dose reduction, Clin. Exp. Ophthalmol. 33 (1) (2005) 53–59. [PubMed: 15670079]

[60]. Lloberas N, Torras J, Alperovich G, Cruzado JM, Giménez-Bonafé P, Herrero-Fresneda I, Franquesa ML, Rama I, Grinyó JM, Different renal toxicity profiles in the association of cyclosporine and tacrolimus with sirolimus in rats, Nephrol. Dial. Transplant. 23 (10) (2008) 3111–3119. [PubMed: 18469305]

[61]. Tsukamoto T, Iyo M, Tani K, Sekine Y, Hashimoto K, Ohashi Y, Suzuki K, Iwata Y, Mori N, The effects of FK506, a specific calcineurin inhibitor, on methamphetamine-induced behavioral change and its sensitization in rats, Psychopharmacology 158 (2) (2001) 107–113. [PubMed: 11702083]

[62]. Li D, Xia Y, Electrospinning of nanofibers: reinventing the wheel? Adv. Mater. 16 (14) (2004) 1151–1170.

[63]. Matter CM, Rozenberg I, Jaschko A, Greutert H, Kurz DJ, Wnendt S, Kuttler B, Joch H, Grünenfelder J, Zünd G, Tanner FC, Lüscher TF, Effects of tacrolimus or sirolimus on proliferation of vascular smooth muscle and endothelial cells, J. Cardiovasc. Pharmacol. 48 (6) (2006) 286–292. [PubMed: 17204907]

[64]. Klawitter J, Nashan B, Christians U, Everolimus and sirolimus in transplantation-related but different, Expert Opin. Drug Saf. 14 (7) (2015) 1055–1070. [PubMed: 25912929]
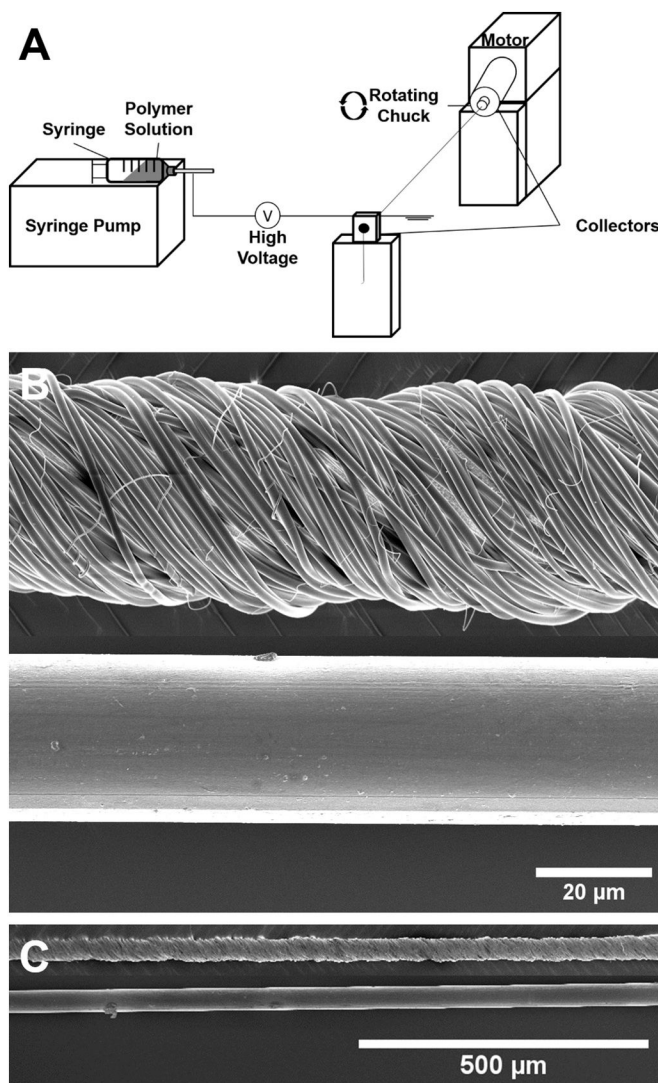
Fig. 1.
Manufacturing schematic and SEM images of nanofiber-coated sutures. (A) Schematic of suture coating system: high voltage was applied to the nozzle of a syringe containing a volatile polymer/drug solution which was pumped at a controlled rate. A standard suture was suspended between two parallel, grounded collectors, where one collector was stationary and one could be mechanically rotated. Following fiber deposition across the collectors, the rotating collector twisted deposited fibers into a uniform coating around the suture. (B) High magnification SEM image of a 10–0 nylon suture coated with nanofibers (top) and a plain 10–0 nylon suture (bottom). (C) Low magnification SEM image showing the uniform nanofiber-coating along the length of the 10–0 nylon suture (top) and a plain 10–0 nylon suture (bottom).
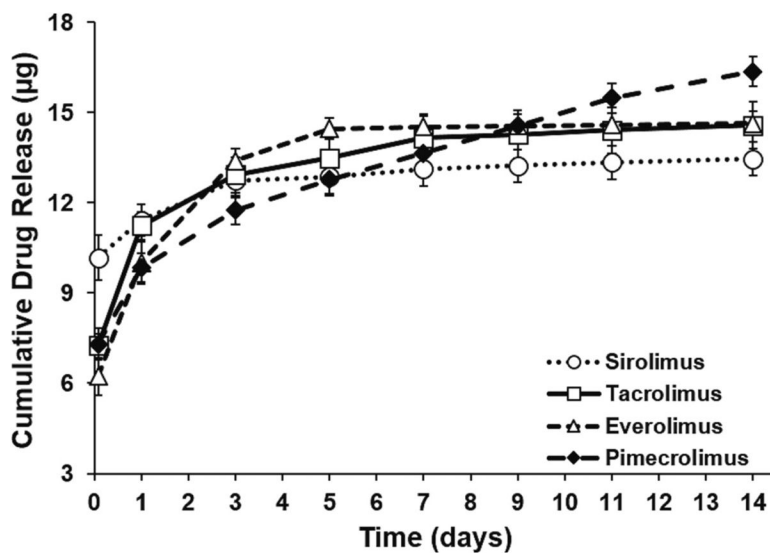
Fig. 2.
Cumulative in vitro release of sirolimus, tacrolimus, everolimus, and pimecrolimus. In vitro release profiles nanofiber bundles composed of 40% (*w*/w) sirolimus, tacrolimus, everolimus, or pimecrolimus (*n* = 4, each) in PLLA/PEG over 14 days. Nanofiber bundles were 5 cm long and 50 μm in diameter.
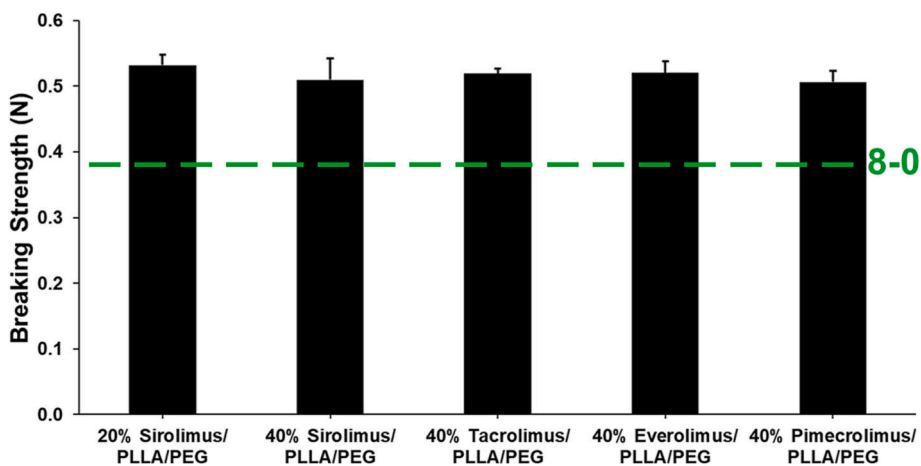
Fig. 3.
Breaking strength of nanofiber-coated nylon sutures in reference to U.S.P. specifications. Comparison of knot-pull breaking strength of 8–0-sized, nylon sutures coated with nanofibers containing 20% or 40% (*w*/w) sirolimus, or 40% tacrolimus, 40% everolimus, or 40% pimecrolimus ($n = 4$, each) in PLLA/PEG. Due to the underlying 10–0 nylon core, there were no significant differences in suture breaking strength observed with increased drug loading or change in drug in the nanofiber coating.
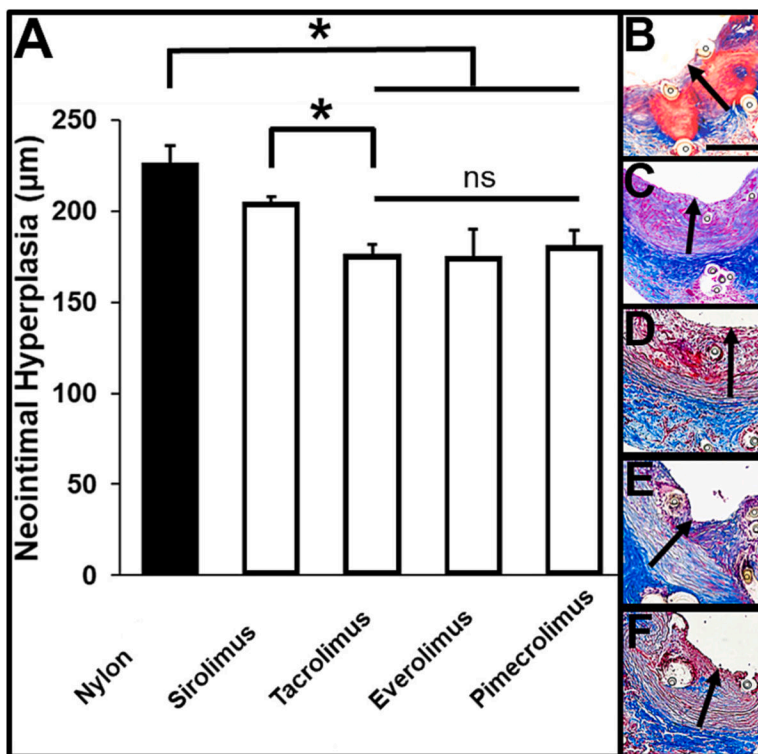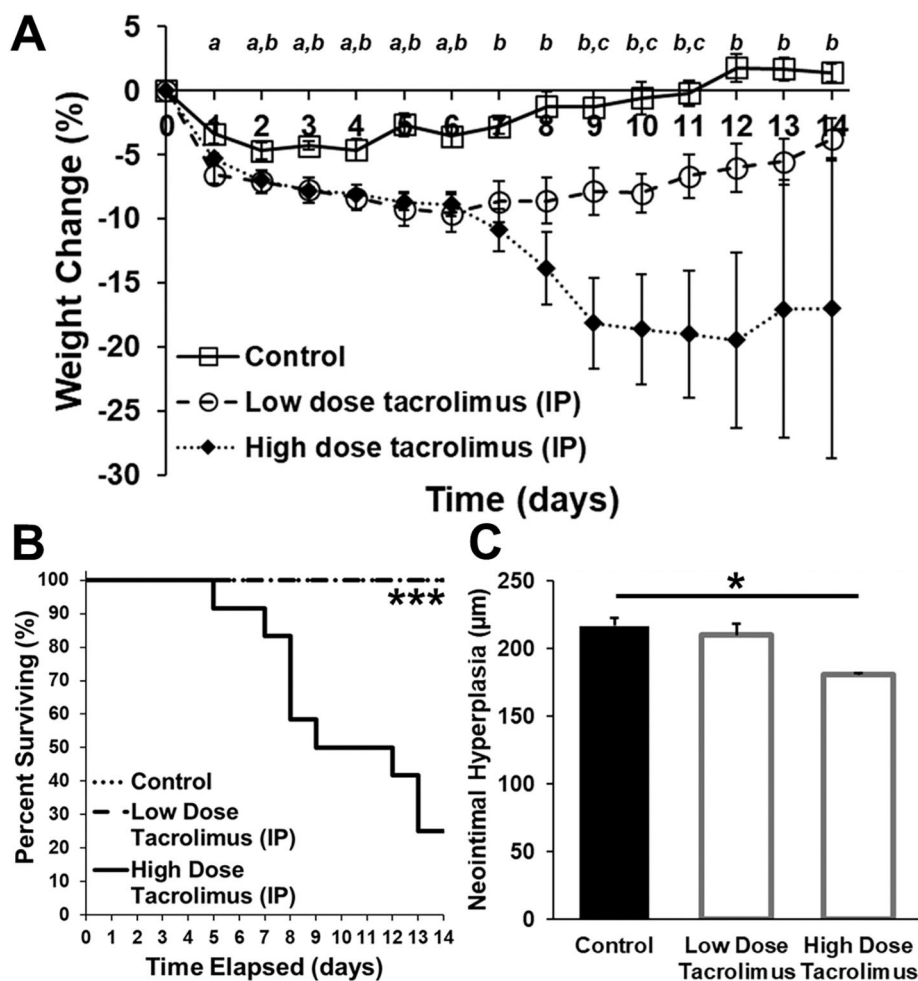
Fig. 4.
Evaluation of neointimal hyperplasia 14 days after vascular anastomosis. (A) Quantification of neointimal hyperplasia, * $p < 0.05$. Representative images of H&*E*-stained tissue sections of rat abdominal aorta 14 days after the anastomosis procedure using 8–0-sized (B) nylon, (C) 40% sirolimus, (D) 40% tacrolimus, (E) 40% everolimus, or (F) 40% pimecrolimus sutures ($n = 6$, each). Drug-eluting sutures had a 10–0 nylon suture core. Black arrows indicate regions of neointimal hyperplasia. ° indicates the cross-section of a suture or the space where a suture existed prior to histology. Scale bar denotes 200 μm.
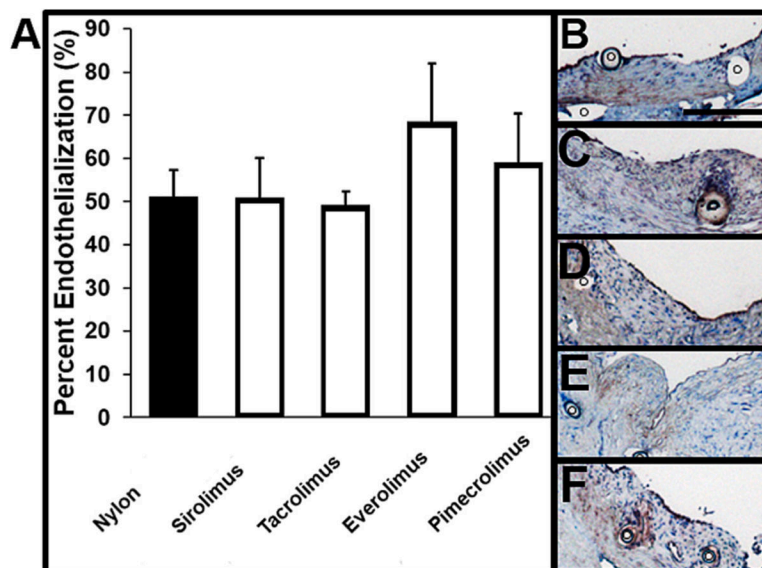
Fig. 5.
Evaluation of vessel endothelialization 14 days after vascular anastomosis. (A)
Quantification of percent of vessel lining that is CD31+ (endothelialization). Representative
images of CD31-stained tissue sections of rat abdominal aorta 14 days after the anastomosis
procedure using 8–0-sized (B) nylon ($n = 6$), (C) 40% sirolimus (n = 6), (D) 40% tacrolimus
($n = 5$), (E) 40% everolimus ($n = 4$), or (F) 40% pimecrolimus (n = 4) sutures. ° indicates the
cross-section of a suture or space where a suture existed prior to histology. Scale bar denotes
200 μm.

Fig. 6.

Evaluation of the safety and efficacy of systemically administered tacrolimus following vascular anastomosis. (A) Daily body weight measurements, (B) percent survival, and (C) quantification of neointimal hyperplasia 14 days after anastomosis of the rat abdominal aorta using 8–0 nylon sutures and daily intraperitoneal administration of 1 mL of vehicle (control; $n = 5$), low dose tacrolimus (1 mg/kg; $n = 6$), or high dose tacrolimus (10 mg/kg; $n = 12$). Body weight changed significantly throughout the post-operative period (*a* indicates a significant difference between control and low dose conditions ($p < 0.05$); *b* indicates a significant difference between control and high dose conditions ($p < 0.05$); *c* indicates a significant difference between low and high dose conditions ($p < 0.05$)). There was a significant difference in survival rate (*** $p < 0.001$) between the groups. Rats in the high dose group had a significant reduction in neointimal hyperplasia in comparison to the control group (* $p < 0.05$), but this was associated with significant weight loss and a 25% survival rate.